Swept optical single sideband modulation for spectral measurement applications using stimulated Brillouin scattering

Mikel Sagues and Alayn Loayssa*

Departamento de Ingeniería Eléctrica y Electrónica, Universidad Pública de Navarra
Campus Arrosadia s/n, 31006 Pamplona, Spain
*alayn.loayssa@unavarra.es
www.unavarra.es

Abstract: We propose a technique for the generation of broadband optical single sideband modulated signals. The technique is based on optically processing an optical double sideband signal using stimulated Brillouin scattering effect. An unwanted sideband suppression over 40 dB in a broadband range from 50 MHz to 20 GHz is experimentally demonstrated. In addition, we apply the generated optical single sideband signal for the spectral characterization of polarization dependent parameters of optical components. The experimental characterization of the polarization dependent loss and the differential group delay of a phase-shifted fiber Bragg grating is performed in order to demonstrate the feasibility of the technique.

OCIS codes: (999.9999) Single sideband modulation; (290.5900) Scattering, stimulated Brillouin; (070.1170) Analog optical signal processing; (070.4340) Nonlinear optical signal processing; (060.4370) Nonlinear optics, fibers; (999.9999) Microwave photonics.

References and links

1. T. Niemi, M. Uusimaa, and H. Ludvigsen, "Limitations of phase-shift method in measuring dense group delay ripple of fiber Bragg gratings," IEEE Photon. Technol. Lett. **13**(12), 1334–1336 (2001).
2. G. D. VanWiggeren, A. R. Motamedi, and D. M. Baney, "Single-Scan Interferometric Component Analyzer," IEEE Photon. Technol. Lett. **15**(2), 263–265 (2003).
3. J. E. Román, M. Y. Frankel, and R. D. Esman, "Spectral characterization of fiber gratings with high resolution," Opt. Lett. **23**(12), 939–941 (1998).
4. R. Hernández, A. Loayssa, and D. Benito, "Optical vector network analysis based on single-sideband modulation," Opt. Eng. **43**(10), 2418–2421 (2004).
5. A. Loayssa, R. Hernández, D. Benito, and S. Galech, "Characterization of stimulated Brillouin scattering spectra by use of optical single-sideband modulation," Opt. Lett. **29**(6), 638–640 (2004).
6. D. J. Krause, J. C. Cartledge, L. Jakober, and K. Roberts, "Measurement of passive optical components using a carrier and single sideband," in Proc. Optical Fiber Communications Conference, (OFC'2006) paper OFN5 (2006).
7. T. Kawanishi, T. Sakamoto, and M. Izutsu, "Optical filter characterization by using optical frequency sweep technique with a single sideband modulator," IEICE Electron. Express **3**(3), 34–38 (2006).
8. D. K. Gifford, B. J. Soller, M. S. Wolfe, and M. E. Froggatt, "Optical vector network analyzer for single-scan measurements of loss, group delay, and polarization mode dispersion," Appl. Opt. **44**(34), 7282–7286 (2005).
9. B. L. Heffner, "Deterministic, analytically complete measurement of polarization dependent transmission through optical devices," IEEE Photon. Technol. Lett. **4**, 451–454 (1992).
10. B. L. Heffner, "Automated Measurement of Polarization Mode Dispersion Using Jones Matrix Eigenanalysis," IEEE Photon. Technol. Lett. **4**,1066–1069 (1992).
11. R. M. Craig, "Accurate Spectral Characterization of Polarization-Dependent Loss," J. Lightwave Technol. **21**(2), 432–437 (2003).
12. P. A. Williams, "Modulation phase-shift measurement of PMD using only four launched polarization states: a new algorithm," Electron. Lett. **35**(18), 1578–1579 (1999).
13. Y. Shi, L. Yan, and X. S. Yao, "Automatic Maximum-Minimum Search Method for Accurate PDL and DOP Characterization," J. Lightwave Technol. **24**(11), 4006–4012 (2006).
14. M. Sagues, M. Pérez, and A. Loayssa, "Measurement of polarization dependent loss, polarization mode dispersion and group delay of optical components using swept optical single sideband modulated signals," Opt. Express **16**(20), 16181–16188 (2008), http://www.opticsinfobase.org/oe/abstract.cfm?URI=oe-16-20-16181.

#130390 - $15.00 USD Received 21 Jun 2010; revised 23 Jul 2010; accepted 24 Jul 2010; published 30 Jul 2010

15. G. H. Smith, D. Novak, and Z. Ahmed, "Technique for optical SSB generation to overcome dispersion penalties in fibre-radio systems," Electron. Lett. **33**(1), 74–75 (1997).
16. T. Fujiwara, and K. Kikushima, "140 Carrier, 20GHz SCM Signal Transmission across 200km SMF by Two-step Sideband Suppression Scheme in Optical SSB Modulation," in Proc. Optical Fiber Communications Conference, (OFC'2007) paper OME2 (2007).
17. K. Takano, N. Hanzawa, S. Tanji, and K. Nakagawa, "Experimental Demonstration of Optically Phase-Shifted SSB Modulation with Fiber-Based Optical Hilbert Transformers," in Proc. Optical Fiber Communications Conference, (OFC'2007) paper JThA48 (2007).
18. K. Higuma, S. Oikawa, Y. Hashimoto, H. Nagata, and M. Izutsu, "X-cut lithium niobate optical single-sideband modulator," Electron. Lett. **37**(8), 515–516 (2001).
19. T. Kawanishi, and M. Izutsu, "Linear single-sideband modulation for high-SNR wavelength conversion," IEEE Photon. Technol. Lett. **16**(6), 1534–1536 (2004).
20. D. Fonseca, A. V. Cartaxo, and P. Monteiro, "Adaptive Optoelectronic Filter for Improved Optical Single Sideband Generation," IEEE Photon. Technol. Lett. **18**(2), 415–417 (2006).
21. H. Kim, "EML-Based Optical Single Sideband Transmitter," IEEE Photon. Technol. Lett. **20**(4), 243–245 (2008).
22. G. P. Agrawal, Nonlinear Fiber Optics (San Diego: Academic Press, 3rd Edition, 2001).
23. X. S. Yao, "Brillouin Selective Sideband Amplification of Microwave Photonic Signals," IEEE Photon. Technol. Lett. **10**(1), 138–141 (1998).
24. Y. Shen, X. Zhang, and K. Chen, "Modulation of 11-GHz RoF system using stimulated Brillouin scattering," IEEE Photon. Technol. Lett. **17**(6), 1277–1279 (2005).
25. M. González Herráez, K.-Y. Song, and L. Thévenaz, "Arbitrary-bandwidth Brillouin slow light in optical fibers," Opt. Express **14**(4), 1395–1400 (2006), http://www.opticsinfobase.org/oe/abstract.cfm?URI=oe-14-4-1395.
26. Z. Zhu, A. M. C. Dawes, D. J. Gauthier, L. Zhang, and A. E. Willner, "12-GHz-Bandwidth SBS slow light in optical fibers," in Proc. Optical Fiber Communications Conference, (OFC'2006), paper PDP1, (2006).
27. M. Sagues, G. Beloki, and A. Loayssa, "Broadband Swept Optical Single-sideband Modulation Generation for Spectral Characterization of Optical Components," European Conference on Optical Communication (ECOC'2007), paper 6.6.6, 2007.
28. W. Kaiser, and M. Maier, "*Stimulated Rayleigh, Brillouin and Raman Spectroscopy*," Laser Handbook, Vol. 2, Chap. E2 (Amsterdam: North-Holland, 1972).
29. M. Sagues, A. Loayssa, and J. Capmany, "Multitap complex-coefficient incoherent microwave photonic filters based on stimulated Brillouin scattering," IEEE Photon. Technol. Lett. **19**(16), 1194–1196 (2007).
30. A. Loayssa, and F. J. Lahoz, "Broad-band RF photonic phase shifter based on stimulated Brillouin scattering and single-sideband modulation," IEEE Photon. Technol. Lett. **18**(1), 208–210 (2006).
31. R. Montgomery, and R. DeSalvo, "A Novel Technique for Double Sideband Suppressed Carrier Modulation of Optical Fields," IEEE Photon. Technol. Lett. **7**(4), 434–436 (1995).
32. M. Nikles, L. Thévenaz, and P. Robert, "Brillouin gain spectrum characterization in single-mode optical fibers," J. Lightwave Technol. **15**(10), 1842–1851 (1997).
33. K. Y. Song, K. S. Abedin, K. Hotate, M. González Herráez, and L. Thévenaz, "Highly efficient Brillouin slow and fast light using As(2)Se(3) chalcogenide fiber," Opt. Express **14**(13), 5860–5865 (2006), http://www.opticsinfobase.org/abstract.cfm?URI=oe-14-13-5860.
34. D. Derickson, *Fiber Optics Test and Measurement* (Prentice Hall PTR, 1998).

Introduction

Currently, a growing number of applications require high-resolution measurement techniques for the spectral characterization of optical components in terms of amplitude and phase-shift responses. Traditionally, two methods have been used for this purpose: the modulation phase-shift method [1] and the interferometric method [2]. The use of optical single sideband (OSSB) modulation has been recently proposed for the spectral characterization of optical components because of the potential that this optical modulation format offers for extremely high wavelength resolution measurements [3–7]. Furthermore, full polarization-resolved measurements of parameters such as polarization dependent loss (PDL) and polarization mode dispersion (PMD) are necessary for the characterization of real-world optical components. A number of techniques have been proposed for the measurement of those parameters [8–13], but none of them yields the spectral resolution that could be achieved with OSSB characterization.

In order to overcome the previous limitation, we have introduced a new OSSB modulation-based characterization technique for the measurement of polarization dependent parameters that allows for very high spectral resolution [14]. However, it has also been found that very high levels of suppression of the unwanted sideband are required in order to achieve sufficient optical phase-shift and amplitude measurement accuracy [4]. In the last years, a number of techniques have been developed for the generation of OSSB signals [15–21].

#130390 - $15.00 USD Received 21 Jun 2010; revised 23 Jul 2010; accepted 24 Jul 2010; published 30 Jul 2010

However, there is a need to enhance the quality of the OSSB signals provided by the existing modulation methods, particularly when broadband modulation is required.

The process of stimulated Brillouin scattering (SBS) can be described as the interaction between two counterpropagating optical waves: a pump wave which controls the gain of a Stokes wave, and a Stokes wave which controls the attenuation of the pump wave [22]. Furthermore, this interaction takes place in a very narrow-bandwidth spectral resonance, with a linewidth of the order of a few tens of MHz, and whose frequency location is controlled by the frequencies of the Stokes and the pump waves. In view of these characteristics, stimulated Brillouin scattering can be a powerful tool to process optical signals, by modifying their magnitude and phase-shift in selected zones of the optical spectrum.

SBS based selected sideband amplification of a modulated optical signal was proposed several years ago for radio over fiber applications [23]. The idea is to process a conventional optical double sideband (ODSB) modulated signal in order to amplify one of the sidebands while the optical carrier and the second sideband remain unaltered. A variation of the previous technique is based on the simultaneous use of Brillouin gain and attenuation processing, so that a sideband of the original ODSB modulated signal is amplified, while the second is attenuated [24]. However, this is a narrowband technique which is limited to modulation frequencies near the Brillouin frequency shift. Therefore, the only way of making a sweep of the modulation frequency of the OSSB signal is by tuning the Brillouin frequency shift of the fiber. This can be done by controlling the temperature or applying strain to the fiber, but in any case the tuning range will be small. Another possibility is to use Brillouin spectrum broadening techniques that allow Brillouin bandwidths of the order of GHz [25,26], but the overall power requirements of the system in order to achieve a significant unwanted sideband suppression ratio will be very high and extra noise will be added to the processing.

Recently, we have introduced a promising novel technique to generate OSSB modulated signals that is also based on processing an ODSB modulated signal using Stimulated Brillouin scattering [27]. In this work, we further develop the technique achieving high quality OSSB modulation with an unwanted sideband suppression over 40 dB in a broadband range from 50 MHz to 20 GHz. This overcomes the limitations of the previously reported schemes enabling a broadband sweep of the modulation frequency and a higher unwanted sideband suppression ratio. In addition, the operation of the modulation technique is theoretically and experimentally investigated to identify the main factors that may constrain its performance. Finally, we demonstrate the feasibility of this modulation scheme to be deployed for the spectral characterization of optical components, including their polarization dependent parameters.

Fundamentals

Figure 1 schematically depicts the principle behind the technique which is based on a double stimulated Brillouin scattering interaction. The idea is to counterpropagate a double-sideband modulated optical carrier at an RF frequency f_{RF} (Fig. 1(a)) with a pump and a Stokes waves in a length of fiber in order to excite SBS effect. The frequency detuning between these signals is set so that the pump wave generates Brillouin gain on one of the sidebands of the ODSB signal while the Stokes wave generates Brillouin loss over the other sideband. Therefore, an OSSB modulated signal is generated as depicted in Fig. 1(b). The gain and attenuation Brillouin processing spectra are also shown in Fig. 1.

Stimulated Brillouin scattering can be described using three coupled differential equations that describe the interaction between the complex amplitudes of the optic fields of the pump and Stokes waves and an acoustic field [28]. Under steady-state conditions, applicable for a continuous wave (CW) or quasi-CW pump and Stokes waves, SBS is governed by two coupled differential equations that describe the intensities of the Stokes and pump waves [22].

#130390 - $15.00 USD Received 21 Jun 2010; revised 23 Jul 2010; accepted 24 Jul 2010; published 30 Jul 2010

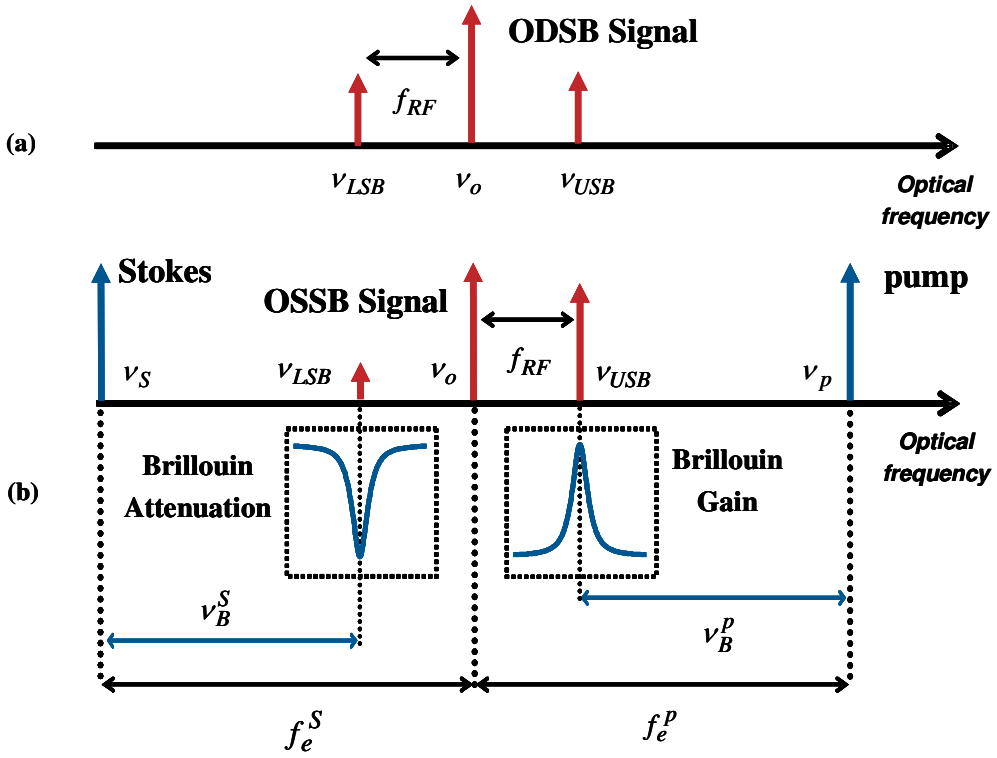

Fig. 1. Fundamentals of the SBS based OSSB modulation technique. SBS processing is performed by counterpropagating pump and Stokes waves (in blue) with an ODSB modulated signal. (a) Unprocessed ODSB signal, (b) OSSB signal obtained by amplification of the upper sideband and attenuation of the lower sideband of the ODSB signal.

In the OSSB modulation scheme described in Fig. 1, we have two simultaneous and independent interactions: one of the sidebands of the ODSB modulated signal interacts with a Stokes wave, acting as a pump wave and suffering attenuation, while the second sideband acts like a Stokes wave interacting with the pump wave, and consequently being amplified.

If OSSB is generated amplifying the upper sideband of the ODSB modulated signal (Fig. 1 (b)), the intensities of that sideband I_{USB} and of the pump wave I_P will be given by:

$$\begin{aligned} \frac{dI_{USB}}{dz} &= g_B\left(\Delta\nu_{USB}\right)\cdot I_P\cdot I_{USB} - \alpha\cdot I_{USB} \\ \frac{dI_P}{dz} &= g_B\left(\Delta\nu_{USB}\right)\cdot I_P\cdot I_{USB} + \alpha\cdot I_P \end{aligned} \tag{1}$$

where α is the attenuation coefficient of the fiber and $g_B(\Delta\nu)$ is the Brillouin gain coefficient that has a Lorentzian dependence given by:

$$g_B\left(\Delta\nu\right) = g_B\frac{\left(\Delta\nu_B/2\right)^2}{\Delta\nu^2+\left(\Delta\nu_B/2\right)^2} \tag{2}$$

where g_B is the Brillouin line center gain factor and $\Delta\nu_B$ is the Brillouin linewidth. In Eq. (1), $\Delta\nu_{USB}=\nu_{USB}-\left(\nu_P-\nu_B^p\right)$ is the detuning of the optical frequency of the sideband we want to amplify ν_{USB}, from the central frequency of the Brillouin gain spectrum, given by the

#130390 - $15.00 USD Received 21 Jun 2010; revised 23 Jul 2010; accepted 24 Jul 2010; published 30 Jul 2010

optical frequency detuning between the pump optical frequency ν_P and the Brillouin frequency shift ν_B^p at the pump wavelength.

The maximum Brillouin interaction (and therefore, the maximum amplification of the sideband) will take place when $\Delta\nu_{USB}=0$, so that:

$$\nu_P = \nu_B^p + \nu_{USB} \tag{3}$$

Substituting $\nu_P = \nu_o + f_e^p$ (with ν_o the optical frequency of the carrier of the ODSB modulated signal and f_e^p the frequency detuning between the carrier and the pump wave) and $\nu_{USB} = \nu_o + f_{RF}$ in Eq. (3), yields:

$$f_e^p = \nu_B^p + f_{RF} \tag{4}$$

In a similar way, the intensities of the lower sideband I_{LSB} and the Stokes wave I_S are related by the following coupled differential equations:

$$\begin{aligned} \frac{dI_{LSB}}{dz} &= -g_B\left(\Delta\nu_{LSB}\right)\cdot I_{LSB}\cdot I_S - \alpha\cdot I_{LSB} \\ \frac{dI_S}{dz} &= -g_B\left(\Delta\nu_{LSB}\right)\cdot I_{LSB}\cdot I_S + \alpha\cdot I_S \end{aligned} \tag{5}$$

where $\Delta\nu_{LSB} = \nu_S - \left(\nu_{LSB} - \nu_B^S\right)$ is the deviation of the optical frequency of the sideband we want to attenuate ν_{USB} from the central frequency of the Brillouin attenuation spectrum, given by the optical frequency detuning between the Stokes wavelength ν_S and the Brillouin frequency shift ν_B^S at the wavelength of the lower sideband ν_{LSB} (pump wave, in this interaction). Therefore, the maximum Brillouin interaction (maximum attenuation of the lower sideband) will take place when:

$$f_e^S = f_{RF} + \nu_B^S \tag{6}$$

with f_e^S the frequency detuning between the optical carrier of the ODSB modulated signal and the Stokes wave. In all the derivations it is assumed that the ODSB signal is injected in the fiber in $z=0$ and travels in the $+z$ direction, while the pump and Stokes waves are injected in $z=L$ and travel in $-z$ direction.

From the previous expressions it is clear that in order to maximize the unwanted sideband suppression of the OSSB signal, the frequency detuning between the pump and Stokes waves and the sidebands of the ODSB modulated signal must coincide with the Brillouin frequency shift of the fiber ν_B at the wavelength of operation. Usually we can assume that the Brillouin frequency shift will be the same for both interactions, provided that the dependency of this parameter is relatively small with wavelength [22]. Therefore, and given that the frequency separation between the optical carrier of the ODSB modulated signal and its two main sidebands is equal, substituting $\nu_B = \nu_B^S = \nu_B^P$ in Eq. (4) and Eq. (6) it can be shown that the frequency separation between the Stokes wave and the optical carrier must be the same as the frequency detuning between the optical carrier and the pump wave:

$$f_e = f_e^S = f_e^p \tag{7}$$

It is easy to obtain the equivalent expressions for the case where we want to amplify the lower sideband, simply by substituting I_{USB} by I_{LSB} in the above derivation. This situation is

#130390 - $15.00 USD Received 21 Jun 2010; revised 23 Jul 2010; accepted 24 Jul 2010; published 30 Jul 2010

schematically depicted in Fig. 2, where two cases are depicted as a function of the relation between f_{RF} and ν_B.

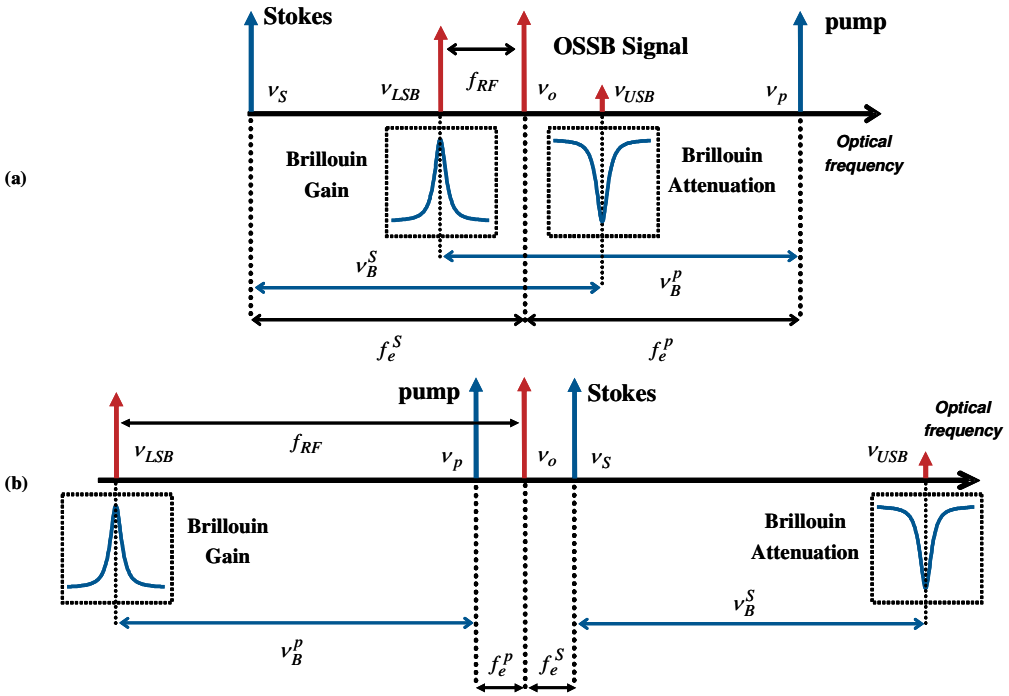

Fig. 2. Fundamentals of the SBS based OSSB modulation technique for the case where the lower sideband is amplified. Two cases are depicted as a function of the relation between f_{RF} and ν_B: (a) $f_{RF} \le \nu_B$ and (b) $f_{RF} \ge \nu_B$. The OSSB signal (in red) is obtained by counterpropagating an ODSB signal with pump and Stokes waves (in blue).

Therefore, in order to adjust the optical frequencies of the different optical components involved in the technique, two cases can be studied: lower sideband amplification and upper sideband amplification. Table 1 shows the proper settings for f_e as a function of f_{RF}, for the two different cases mentioned and for the case where f_{RF} is larger or smaller than ν_B.

Table 1. Frequency separation f_e.

OSSB	$f_{RF} \le \nu_B$	$f_{RF} \ge \nu_B$
Upper sideband amplification (in optical frequency)	$f_e = \nu_B + f_{RF}$	
Lower sideband amplification (in optical frequency)	$f_e = \nu_B - f_{RF}$	$f_e = f_{RF} - \nu_B$

Optimum setting for the frequency separation between the optical carrier of the ODSB modulated signal and the pump and Stokes waves as a function of the RF modulation frequency and the Brillouin frequency shift, in order to generate an OSSB modulated signal.

A key feature of this OSSB modulation scheme is that it allows a tuning of the RF modulation frequency, so that it is possible to perform a sweep of the optical frequency of the

#130390 - $15.00 USD Received 21 Jun 2010; revised 23 Jul 2010; accepted 24 Jul 2010; published 30 Jul 2010

sideband. Furthermore, due to the low bandwidth of Brillouin interaction, the technique can operate from extremely low frequencies. On the other side, the upper limit for the modulation frequency is only limited by the bandwidth of the ODSB modulator and by the way the Stokes and pump waves are generated.

Simulations

Figure 3 shows simulation results for the amplification and attenuation of the sidebands of the ODSB modulated signal as a function of pump and Stokes power. It can be seen that both the amplification and attenuation increase as the pump and Stokes waves power are higher, what will lead to increasing unwanted sideband suppression ratios as the pump and Stokes power is raised. Figure 4 shows the unwanted sideband suppression ratio as a function of pump and Stokes power and of the ODSB signal's sideband power.

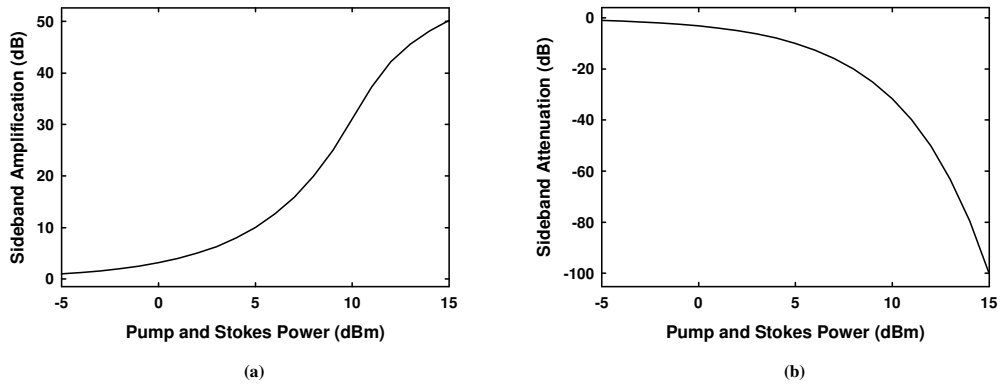

Fig. 3. (a) Sideband amplification and (b) sideband attenuation as a function of pump and Stokes power. Sideband power of the ODSB signal is set to −33 dBm.

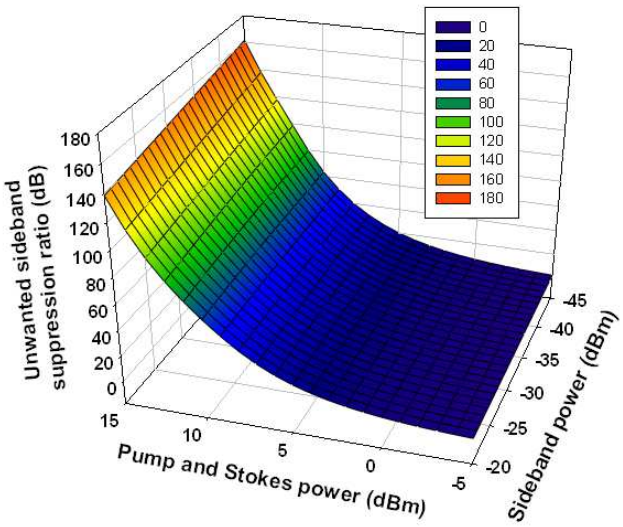

Fig. 4. Unwanted sideband suppression ratio as a function of pump and Stokes power and of sideband power.

In Fig. 4 only SBS interaction has been taking into account when calculating the unwanted sideband suppression ratio that would be achieved. It is important to notice that other nonlinear effects could limit the performance of the system for very high pump and Stokes

#130390 - $15.00 USD Received 21 Jun 2010; revised 23 Jul 2010; accepted 24 Jul 2010; published 30 Jul 2010

powers. For example, Rayleigh scattering could lead to interferences between the OSSB signal and the backscattered pump and Stokes waves for some given RF modulation frequencies. However, from these simulations, very high unwanted sideband suppression ratios can be expected for relatively small pump and Stokes waves powers, what should limit the undesired effect of other nonlinear effects.

However, for very high modulation frequencies, the dependency of ν_B with wavelength should be taken into account. In that case, the unwanted sideband suppression ratio will not be maximized in the full span of the modulation sweep due to the fact that the approximation $\nu_B = \nu_B^S = \nu_B^P$ (and therefore, Eq. (7)) will not be fulfilled as the modulation frequency increases. The frequency dependence of the Brillouin frequency shift is given by [22]:

$$\nu_B = \frac{2 \cdot n \cdot \nu_A}{c} \cdot \nu_p \tag{8}$$

where n is the refraction index of the fiber, c is the speed of light, ν_p is the optical frequency of the pump wave and ν_A is the frequency of the acoustic wave which can be regarded as constant for a given optic fiber [29].

Figure 5 shows the unwanted sideband suppression ratio as a function of the modulation frequency f_{RF} for the case where the lower sideband is amplified (Fig. 2) and for the case where the upper sideband is amplified (Fig. 1). In both cases f_e was calculated from Table 1 taking ν_B as the Brillouin frequency shift of the fiber at the optical frequency of the modulation carrier ν_o. The figure shows that for a 40 GHz modulation frequency sweep the variation of the unwanted sideband suppression ratio is smaller than 0.5 dB (lower sideband amplification) and 0.8 dB (upper sideband amplification). As expected from Table 1, the variation is larger in the latter case, due to the fact that the frequency detuning of the two pump waves involved in the processing is higher when the upper sideband is amplified. However, in both cases the variation can be regarded as negligible comparing to the magnitude of the achieved unwanted sideband suppression ratio.

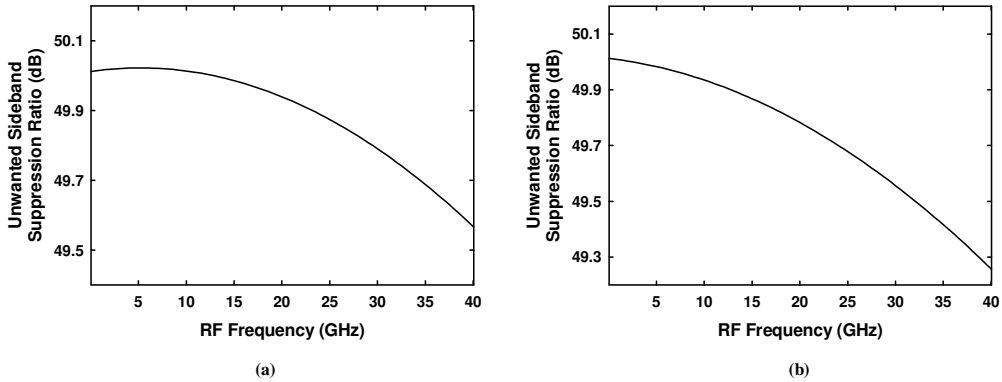

Fig. 5. Unwanted sideband suppression ratio as a function of RF modulation frequency of the ODSB signal. (a) Lower sideband amplification (Fig. 2) and (b) upper sideband amplification (Fig. 1). The pump and Stokes waves power at the input of the fiber was 9 dBm, and the sideband power of the ODSB signal at the input of the fiber was −33 dBm.

All the previous simulations where performed for a 20 km standard singlemode fiber (S-SMF) with an attenuation coefficient of $\alpha = 0.27\,\text{dB/km}$, a Brillouin line center gain factor of $g_B = 1.2 \cdot 10^{-11}\,\text{m/W}$ and a Brillouin linewidth of $\Delta\nu_B = 40\,\text{MHz}$.

#130390 - $15.00 USD Received 21 Jun 2010; revised 23 Jul 2010; accepted 24 Jul 2010; published 30 Jul 2010

Experimental setup and measurements

OSSB Generation

Due to the narrow bandwidth of SBS interaction, the accurate frequency tuning of all the optical waves involved in the technique described above is of paramount importance. The experimental setup used to demonstrate the technique is schematically depicted in Fig. 6, where all the optical waves are generated from a single laser source, so that the latter requirement is easily satisfied. This setup is based on the one that we have recently developed for optical signal processing using SBS nonlinear effect [30].

The output of a laser source is divided in two paths by a fiber optic coupler. The lower path goes to a conventional Mach Zehnder electrooptic modulator (MZ-EOM) driven by an RF signal of frequency f_{RF}, generating an ODSB modulated signal. In order to have a pump wave and a Stokes wave equally detuned from the optical carrier (as requires according to Eq. (7)), the upper path goes to another MZ-EOM, which is driven by a microwave signal generator of frequency f_e and biased for minimum transmission, so that an optical double-sideband suppressed-carrier (ODSB-SC) signal is generated [31]. A circulator is used to counterpropagate the signals of both branches in a 20 km length of S-SMF. Following the principle schematically depicted in Fig. 1 and Fig. 2, for a given f_{RF} the modulation frequency of the ODSB-SC modulator f_e is set so that SBS interaction takes place between the two main sidebands of the ODSB-SC signal (which act as pump and Stokes waves) and the sidebands of the ODSB modulated signal. For each RF modulation frequency, f_e must be set following the values given in Table 1 in order to maximize the unwanted sideband suppression ratio of the modulation. Therefore, the Brillouin frequency shift at the wavelength of operation of the fiber must be accurately measured using any of the techniques available in the literature [5,32]. The fiber deployed in the experiment had a Brillouin frequency shift of 10.882 GHz at a pump wavelength of 1552.95 nm. The required length of fiber will be a function of the power of the pump and Stokes waves and of the Brillouin gain coefficient of the deployed fiber. Therefore, highly nonlinear fiber with a very high Brillouin gain coefficient could also be deployed to reduce the length of fiber needed [33]. In our setup an EDFA is used to amplify the ODSB-SC signal so that the required power to excite SBS effect is achieved.

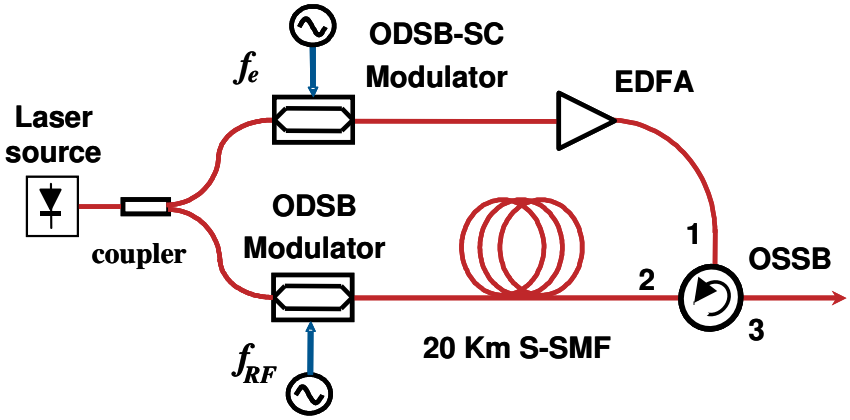

Fig. 6. Experimental setup of the OSSB modulator.

#130390 - $15.00 USD Received 21 Jun 2010; revised 23 Jul 2010; accepted 24 Jul 2010; published 30 Jul 2010

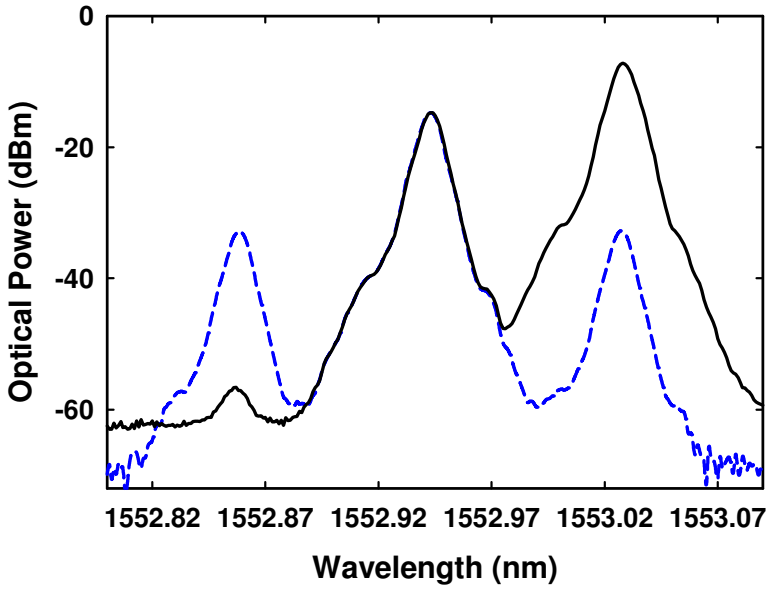

Fig. 7. Optical spectrum of the OSSB signal (black solid line) and the original ODSB signal (blue dashed line) for a 10.5 GHz modulation frequency.

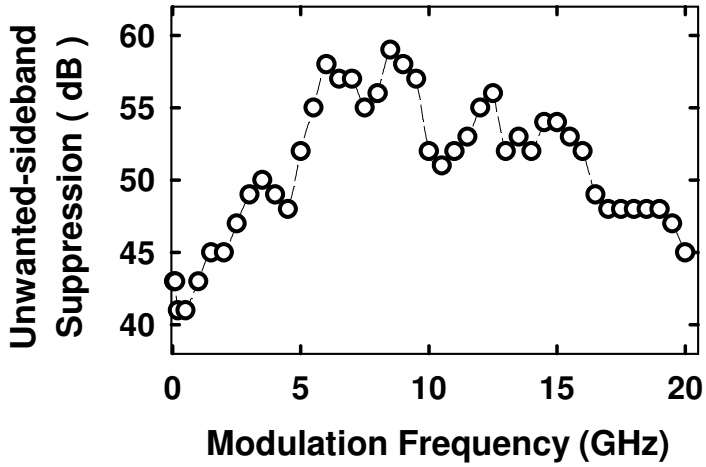

Fig. 8. Unwanted sideband suppression as a function of the modulation frequency f_{RF} of the OSSB signal.

Figure 7 shows the optical spectrum of the OSSB modulated signal generated with the proposed technique for a frequency modulation of 10.5 GHz (solid line) and the original ODSB modulated signal (dashed blue line), measured in a 10-pm resolution optical spectrum analyzer (OSA). An unwanted sideband suppression ratio above 50 dB can be observed.

Figure 8 depicts the unwanted sideband suppression ratio as a function of the modulation frequency f_{RF}. The measurement from 6.5 GHz to 20 GHz was performed using a 10-pm resolution OSA and measurements for frequencies below 6.5 GHz were made by heterodyne analysis [34] using an electrical spectrum analyzer. More than 40 dB of suppression was achieved in the range from 50 MHz to 20 GHz. The higher frequency of operation was limited to 20 GHz by the RF modulation bandwidth of the available MZ-EOM and the frequency

#130390 - $15.00 USD Received 21 Jun 2010; revised 23 Jul 2010; accepted 24 Jul 2010; published 30 Jul 2010

range of the EVNA, but in principle the technique should be feasible at arbitrarily high frequencies. Variations in the achieved unwanted sideband suppression ratio are attributed to variations on the power of the counterpropagated signals as a function of the modulation frequency due to the frequency response of the modulators. On top of that, for modulation frequencies above 10 GHz the noise floor level of the OSA was above the power of the attenuated sideband, so that the latter could not be measured accurately. Therefore, for those modulation frequencies the real unwanted sideband suppression ratio will be even higher than shown in Fig. 8.

Application to the characterization of optical components

The use of OSSB signals for spectral characterization applications has been under development for several years [3–7,14]. This technique is based on the correspondence or mapping that this modulation format provides between the optical and the electrical domain. A possible implementation of this method is depicted in Fig. 9 [4]. The optical field at the output of the OSSB modulator can be expressed as:

$$E_{in}(t) = A_o \cdot e^{j2\pi\nu_o t} + A_{SB} \cdot e^{j2\pi(\nu_o + f_{RF})t} \tag{9}$$

where ν_o is the frequency of the optical carrier and $A_o = |A_o| \cdot e^{j\varphi_o}$ and $A_{SB} = |A_{SB}| \cdot e^{j\varphi_{SB}}$ are the complex amplitudes of the optical carrier and sideband, respectively. The generated OSSB modulated signal is propagated though the optical component we want to characterize, which has an optical transfer function $H(\nu)$. Finally, the signal is detected in a wideband photodetector (PD), where the component of the electrical current at f_{RF} is found to be proportional to [4]:

$$\begin{aligned} i_{out}(t)|_{f=f_{RF}} \propto & |A_o| \cdot |A_{SB}| \cdot |H(\nu_o)| \cdot |H(\nu_o + f_{RF})| \times \\ & \times \cos\left(2\pi f_{RF} t - \phi_o + \phi_{SB} - \arg\left(H(\nu_o)\right) + \arg\left(H(\nu_o + f_{RF})\right)\right) \end{aligned} \tag{10}$$

From Eq. (10) it can be shown that from the amplitude and phase-shift of the detected electrical signal it is possible to extract the optical transfer function of the device under test (DUT) at the sideband frequency f_{RF}. Therefore, if the modulation frequency f_{RF} of the OSSB modulated signal is swept, while ν_o is kept constant, and the output RF signal is detected using an electrical vector network analyzer (EVNA), the optical transfer function of the DUT will be recovered in the EVNA [3,4].

In order to demonstrate the feasibility of the OSSB modulation scheme for the spectral characterization of optical components, we have performed an example measurement of the transfer function of a phase-shifted fiber Bragg grating (PS-FBG). The modulating electrical signal at f_{RF} frequency was generated using a 20 GHz bandwidth EVNA, while the modulating signal on the upper branch at frequency f_e was generated with a signal generator. Both instruments and the tunable laser where controlled using a computer through GPIB interface in order to set the wavelength of the optical carrier and to synchronize the modulation frequencies feeding the optical modulators according to Table 1.

#130390 - $15.00 USD Received 21 Jun 2010; revised 23 Jul 2010; accepted 24 Jul 2010; published 30 Jul 2010

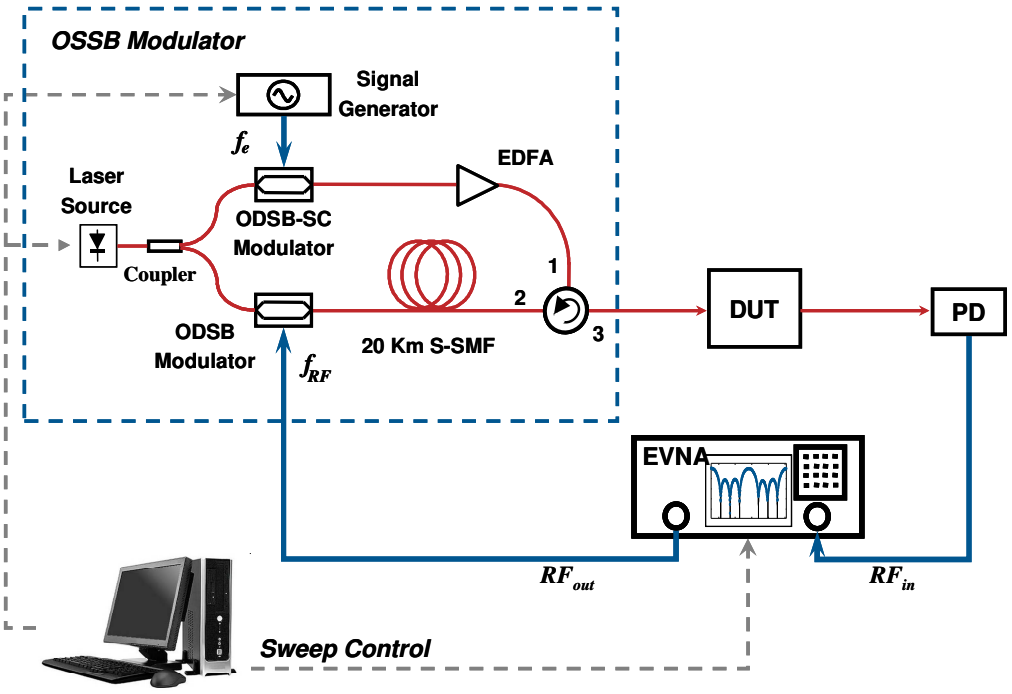

Fig. 9. Experimental setup for the characterization of optical components, using the SBS based OSSB modulator.

Figure 10 depicts the optical amplitude and phase-shift characterization of the reflection transfer function of the PS-FBG (solid line). The frequency step in the EVNA was set to 10 MHz. However, the nominal resolution of the measurement can be arbitrarily reduced by reducing this step. The ultimate resolution limit is given by the linewidth of the deployed optical source and by its wavelength stability, which in our setup were lower than 100 kHz and 1 pm/24 hours, respectively. In order to cover the total span of the measurement (over 43 GHz) three partially overlapped sweeps were performed tuning the laser source at different optical frequencies. For the amplitude we also show the 10-pm resolution transfer function measured combining a white source and an OSA (symbols). The small deviation between both measurements is attributed to the polarization dependence of the PS-FBG. Note that the measurement in the OSA can be regarded as polarization-averaged due to the unpolarized light emitted by the deployed white source. However, the measurement performed with the OSSB technique is affected by the polarization-dependence of the characterized component [14]. This particular PS-FBG is found to be a polarization-sensitive component, especially in the optical frequency range where the phase-shift is located, corresponding to the steep notch in its amplitude response.

In order to measure that polarization dependence, the OSSB modulation scheme was used in combination with a novel technique based on OSSB modulation for the measurement of polarization dependent parameters that we have reported recently [14]. This technique is based on sequentially generating two OSSB modulation sweeps with orthogonal linear states of polarization and, for each one, analyzing two orthogonal polarizations at the output of the device under test using a polarization beam splitter. Figure 11 shows the characterization of the polarization dependent loss and the differential group delay (DGD) of the PS-FBG. A 17-GHz optical frequency sweep was performed, centered at the notch of the PS-FBG, with 20-MHz resolution. Measurements using the OSSB method (red solid line) are compared to those using the modulation phase-shift method (black symbols) with 2-pm resolution and 125-MHz frequency modulation [11,12]. Both measurements show good agreement. The small

#130390 - $15.00 USD Received 21 Jun 2010; revised 23 Jul 2010; accepted 24 Jul 2010; published 30 Jul 2010

deviations are attributed to the lower resolution of the modulation phase-shift method and also to the residual PDL and PMD of the available components in the experimental setup.

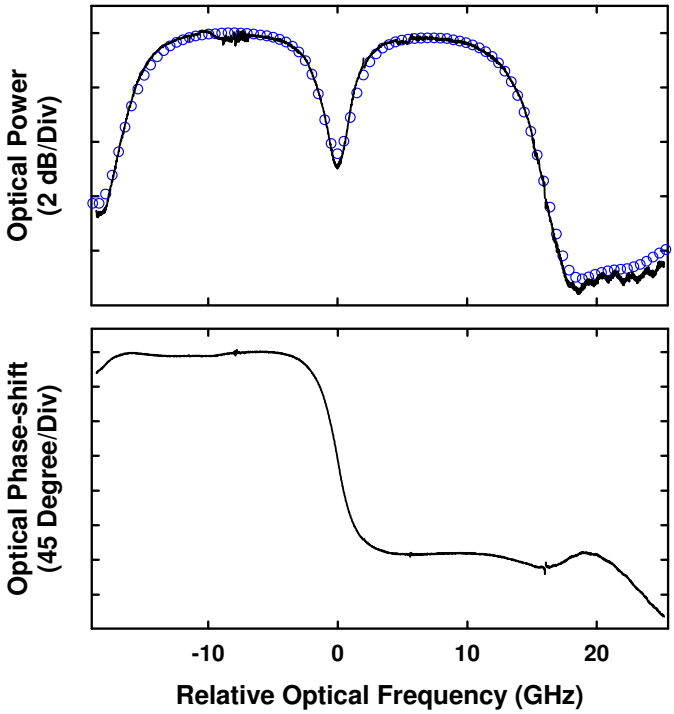

Fig. 10. Amplitude and phase-shift spectral characterization of a PS-FBG using the OSSB modulation technique introduced in the paper. For the amplitude, a lower frequency resolution measurement done with a commercial OSA is also shown (symbols).

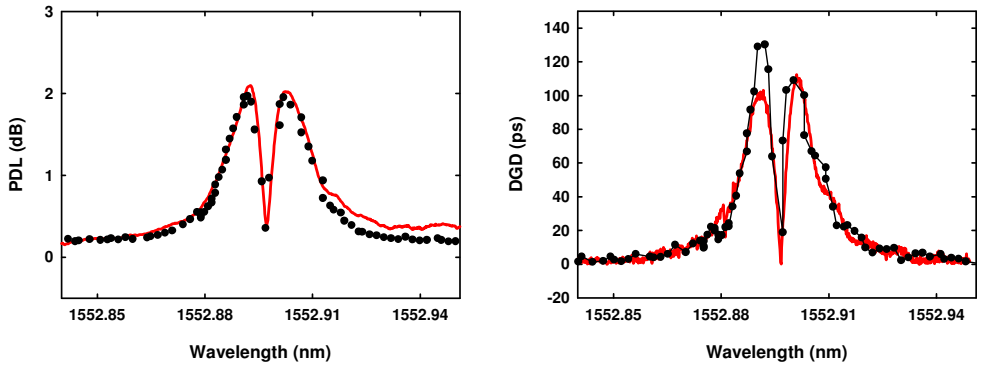

Fig. 11. Characterization of the PDL and DGD of the PS-FBG using the OSSB technique (red solid line) and the modulation phase-shift method (black symbols).

In the measurement setup, reflections in connectors and Rayleigh scattering of the ODSB-SC signal in the fiber could lead to coherent interference in the receiver. It was found that these reflections affected the measurement for some given frequencies. Specifically, for the case where OSSB is generated by amplification of the lower frequency sideband, interferences can be produced for three particular frequencies: when the reflections are located exactly at the same frequency as the sidebands of the OSSB signal:

#130390 - $15.00 USD Received 21 Jun 2010; revised 23 Jul 2010; accepted 24 Jul 2010; published 30 Jul 2010

$$f_{RF} = f_e = \frac{\nu_B}{2} \tag{11}$$

when the reflected optical components are detuned by the modulation frequency f_{RF}, so that their beating at the receiver interferes with the RF component of the detected OSSB signal at the modulation frequency f_{RF}:

$$f_{RF} = 2 \cdot f_e = \frac{2 \cdot \nu_B}{3} \tag{12}$$

$$f_{RF} = 2 \cdot f_e = 2 \cdot \nu_B \tag{13}$$

and in the cases where reflections affect the optical carrier:

$$f_{RF} = \nu_B \Rightarrow f_e = 0 \tag{14}$$

On the other hand, if the OSSB modulated signal is generated by amplification of the upper frequency sideband, there is a single modulation frequency that can lead to interference in the detector. This takes place when the amplified sideband is beaten with the pump wave generating an RF component at the modulation frequency f_{RF}:

$$f_{RF} = \nu_B = \nu_P - \nu_{USB} \tag{15}$$

Finally, another possible source of interference in the measurement are the optical components generated by amplification of the ASE noise by SBS interaction with the Stokes wave, that can lead to electrical interference when these optical components are detuned from the rest of the optical components by the modulation frequency f_{RF}.

To avoid all this possible interferences, a second EDFA was used in the lower branch of the OSSB modulation scheme in order to increase the power of the ODSB signal, so that the interference was reduced. In addition, the particular optical frequencies where interference could be a problem were avoided. Nevertheless, this drawback could be overcome using a highly nonlinear fiber which could provide the same amount of Brillouin scattering effect with less reflections or by further raising the power in the lower branch [33].

Conclusions

A novel SBS based swept OSSB modulation generation technique has been proposed and theoretically studied. Simulation results are very promising, showing that very high unwanted sideband suppression ratios can be achieved with relatively low optical powers.

Experiments have been performed, demonstrating what to our knowledge is the best broadband unwanted sideband suppression ratio reported to date (>40 dB for a frequency range of 20 GHz). In addition, the feasibility of the technique for high accuracy and frequency resolution characterization of optical components has been proved, including the polarization dependent parameters of the components.

In this paper we generate an OSSB signal by processing an ODSB modulated signal. However, the same processing could be applied to enhance the unwanted sideband suppression ratio of an OSSB signal generated my means of any other method [6,7,15–21]. This would increment the complexity of the system, but would reduce the amount of SBS interaction required to achieve a significant sideband suppression ratio. Therefore, the power requirements of the system would be reduced, which could lead to an improvement in the overall noise performance of the system.

Acknowledgements

The authors wish to acknowledge the financial support from the Spanish Ministerio de Educación y Ciencia through the projects TEC2007-67987-C02-02 and TEC2010-20224-C02-01.

#130390 - $15.00 USD Received 21 Jun 2010; revised 23 Jul 2010; accepted 24 Jul 2010; published 30 Jul 2010